

# Compact efficient broadband grating coupler for silicon-on-insulator waveguides

Dirk Taillaert, Peter Bienstman, and Roel Baets

Department of Information Technology, Ghent University, Interuniversity Microelectronics Center, St.-Pietersnieuwstraat 41, 9000 Gent, Belgium

Received March 9, 2004

We have designed a high-efficiency broadband grating coupler for coupling between silicon-on-insulator (SOI) waveguides and optical fibers. The grating is only 13  $\mu\text{m}$  long and 12  $\mu\text{m}$  wide, and the size of the grooves is optimized numerically. For TE polarization the coupling loss to single-mode fiber is below 1 dB over a 35-nm wavelength range when using SOI with a two-pair bottom reflector. The tolerances to fabrication errors are also calculated. © 2004 Optical Society of America

OCIS codes: 130.0130, 050.2770.

Silicon on insulator (SOI) is an interesting material for high-density photonic integrated circuits because of the high refractive-index contrast. One of the challenges is coupling light between optical fibers and SOI waveguides. Because the silicon core layer is only a few hundred nanometers thick, there is a huge mismatch between the waveguide mode and a single-mode fiber mode. This coupling problem is important, and recently several groups demonstrated<sup>1,2</sup> coupling losses below 1 dB using an inverted lateral taper with a polymer overlay. Although this is a good solution to the coupling problem, it would be interesting to have a coupler that can be placed anywhere on a chip and not only at the edges. Such a coupler does not require polishing of facets and allows wafer scale testing of photonic integrated circuits. Grating couplers can do this, but current grating couplers are either efficient<sup>3</sup> or broadband<sup>4</sup> but not both. In this Letter we present a new design that promises a coupling loss below 1 dB over a 35-nm wavelength range for TE polarization. We achieve a large bandwidth by using a short grating with a large coupling strength.

The problem considered is shown in cross section in Fig. 1. The SOI waveguide consists of a 220-nm-thick silicon core on top of a buried oxide layer on a silicon substrate. A grating is etched into the silicon core layer and the grating grooves are invariant in the  $x$  direction, but the SOI waveguide has a finite width. On top of the silicon there is an index-matching layer. The end facet of the fiber is close to the grating, and the fiber is slightly tilted. The angle between the fiber axis and the  $y$  axis is called  $\theta$ , and in the rest of this Letter angle  $\theta$  will be  $8^\circ$ . This value is chosen because it is sufficient to avoid reflection at the waveguide grating and because the angle is small; the approximation  $\cos(\theta) = 1$  can be used in some calculations.

The complete problem is a three-dimensional problem, but it can be reduced to two two-dimensional (2-D) problems because the width of the SOI waveguide is much larger than the height. In Fig. 2 the fundamental TE mode of a 12- $\mu\text{m}$ -wide SOI strip waveguide is shown. Because of the large width of the waveguide, it is a good approximation<sup>5</sup> to write the field  $\psi(x, y)$  as  $\psi_1(x)\psi_2(y)$ , where  $\psi_2(y)$  represents a field component

of the slab mode and  $\psi_1(x)$  is a lateral mode profile. The validity of this approximation is confirmed by the fact that the effective index of the strip waveguide mode calculated with a fully vectorial mode solver (2.8302) is almost identical to the effective index of the SOI slab mode (2.8309). Therefore we consider only the 2-D grating problem in the  $(y, z)$  plane for TE polarization, as is done in most of the grating coupler literature. To calculate the 2-D grating coupler, we use the eigenmode expansion method with perfectly matched layer boundary conditions.<sup>4,6</sup> This rigorous method yields electromagnetic fields  $F(y, z)$  when the normalized slab waveguide mode with power 1 is incident on the grating; thus the coupler is calculated as an output coupler. The coupling efficiency to the fiber is then calculated with the following integral<sup>7</sup>:

$$\eta = \left| \int_S \mathbf{E} \times \mathbf{H}_{\text{fib}}^* dS \right|^2, \quad (1)$$

where the fiber mode is normalized and surface  $S$  is the facet of the fiber. This formula is exact only in uniform media, but it is accurate here because of the index-matching layer and the fact that a fiber is a weakly guiding structure. To calculate this integral, the fiber mode is approximated by a Gaussian beam with a beam diameter of  $2w_0 = 10.4 \mu\text{m}$ , and field  $F(y, z)$  resulting from the 2-D grating calculation is multiplied by  $\psi_1(x)$  to take into account the lateral direction. When neglecting the smaller field components, taking into account that  $\cos(\theta) \approx 1$ , and neglecting the beam divergence in the lateral direction, Eq. (1)

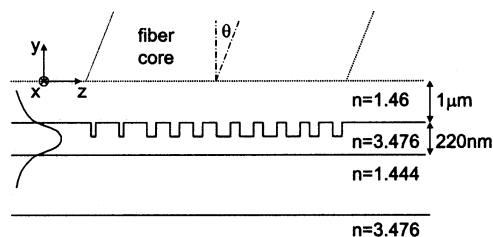


Fig. 1. SOI grating coupler problem.

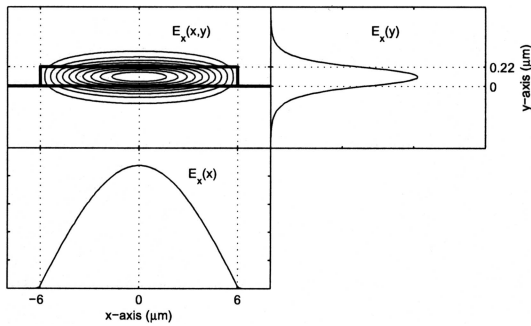


Fig. 2. Fundamental TE mode of a 12- $\mu\text{m}$ -wide SOI strip waveguide.  $E_x(x, y) \approx E_x(x)E_x(y)$ .

can be further simplified to

$$\eta = \left| \int E(x)E(y=0, z)A \exp\left[-\frac{(x-x_0)^2 + (z-z_0)^2}{w_0^2}\right] \times \exp\left(jn_{\text{fib}} \frac{2\pi}{\lambda} z \sin \theta\right) dx dz \right|^2. \quad (2)$$

Constant  $A$  represents the normalization of the Gaussian beam and  $n_{\text{fib}} = 1.46$ . Equation (2) can be separated into two terms, one dependent on  $x$  and the other dependent on  $z$ . If we call the  $x$ -dependent term  $\xi$ , the coupling efficiency to the fiber is the coupling efficiency of a 2-D problem multiplied by correction factor  $\xi$ . For a 12- $\mu\text{m}$ -wide SOI strip waveguide we calculated  $\xi = 0.97$ . In this Letter overlap integral (2) is calculated as a one-dimensional overlap integral multiplied by  $\xi$ .

A grating coupler with a uniform grating can have a maximum theoretical<sup>3</sup> coupling efficiency of approximately 80% because the output beam has exponentially decaying power  $P = P_0 \exp(-2\alpha z)$  along the propagation direction.  $\alpha$  is called the leakage factor or coupling strength of the grating. For a nonuniform grating,  $\alpha$  becomes a function of  $z$  and the output beam can be shaped differently. To achieve a Gaussian output beam,  $\alpha(z)$  is given<sup>8,9</sup> by

$$2\alpha(z) = \frac{G^2(z)}{1 - \int_0^z G^2(t) dt}, \quad (3)$$

where  $G(z)$  is a normalized Gaussian profile. To achieve this  $z$  dependence of  $\alpha$ , either the etch depth<sup>8</sup> or the duty cycle<sup>9</sup> of the grating can be varied. In Fig. 3,  $G^2(z)$  and the corresponding theoretical  $\alpha(z)$  are plotted for a Gaussian beam with a beam diameter of 10.4  $\mu\text{m}$ . It should be noted that Eq. (3) is exact only for a long grating with small  $\alpha$ , which is not the case for our structure. Therefore we use the results of Eq. (3) as a starting point and do a further numerical optimization of the grating structure. We will now discuss our design procedure in more detail. On the basis of the maximum coupling strength that is needed, the etch depth is chosen. A grating period is chosen so that the output beam has the desired angle  $\theta$ . For this etch depth and period,  $\alpha$  is

calculated for different duty cycles. On the basis of these results, the groove widths are chosen to match  $\alpha(z)$  from Fig. 3. The resulting structure, however, has an output beam that has only 75% overlap with  $G(z)$  instead of the 100% expected. The main reason for this is that, because of the large coupling strength, not only is the coupling strength dependent on the duty cycle but the phase difference between two grating teeth is also. As a result, the output field has a more-or-less Gaussian amplitude but a curved phase front. By changing the spacing between the grating teeth, we can correct this phase mismatch. A second reason is that Eq. (3) is accurate only for small  $\alpha$ . Therefore we have decided to numerically optimize the structure to achieve a maximum coupling efficiency to the fiber. We define the grating as 20 groove widths and 19 spacing widths and use a simple genetic algorithm<sup>10</sup> for the optimization. The groove widths and the spacings between the grooves are allowed to change in steps of 5 nm. As a result of this optimization, the overlap with a Gaussian profile is increased from 75% to 97%. The resulting output after optimization is also drawn on Fig. 3, next to the theoretical Gaussian profile.

For a SOI waveguide we have repeated this procedure for different thicknesses of the buried oxide layer, because the thickness of this layer has a major influence on the coupling strength and efficiency.<sup>11</sup> For the structure with optimized buried oxide thickness (925 nm) the maximum coupling efficiency to fiber is 61%. The efficiency versus wavelength is shown in Fig. 4. The efficiency is limited because approximately 35% of the light is lost to the substrate. The efficiency can be further improved by use of SOI with a bottom reflector. For SOI with a two-pair distributed Bragg reflector<sup>12</sup> under the waveguide the maximum coupling efficiency after optimization is 92%. In this structure, only 2% is lost to the substrate. The other 98% is coupled upward, but there is still a small mismatch with the fiber mode, which results in a 92% coupling efficiency to the fiber ( $0.92 = 0.98 \times 0.97 \times \xi$ ). The optimal structure is shown in Fig. 5 together with a field plot. The

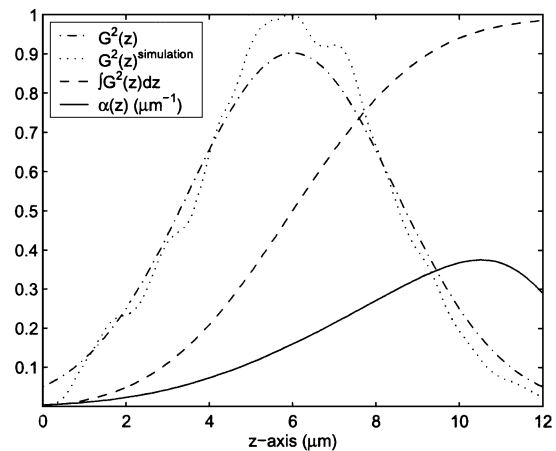


Fig. 3. Gaussian output beam and corresponding  $\alpha(z)$  calculated according to Eq. (3). The dotted curve is the resulting output from the simulation after optimization.

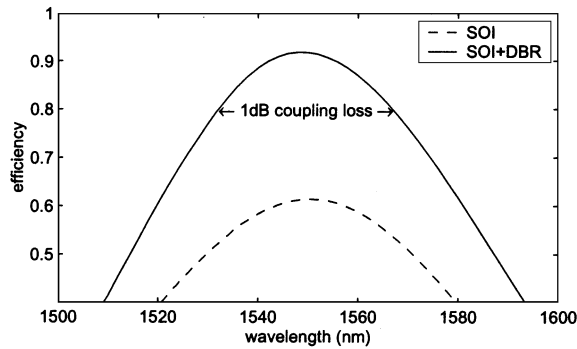


Fig. 4. Coupling efficiency to the fiber for the coupler in a SOI waveguide and SOI waveguide with a bottom reflector, DBR, distributed Bragg reflector.

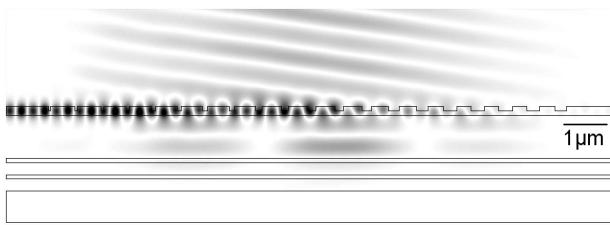


Fig. 5. SOI coupler with a bottom reflector. The plotted field is the real part of  $E_x$ .

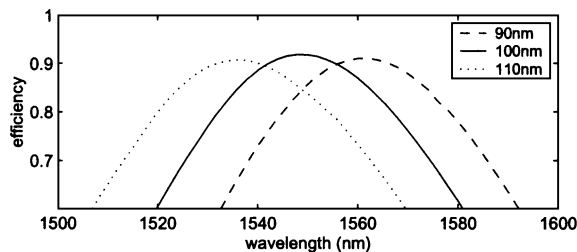


Fig. 6. Coupling efficiency for different etch depths.

smallest groove width is 30 nm. The coupling loss to the fiber for this structure is less than 1 dB in the wavelength range 1532–1567 nm (see Fig. 4). In this wavelength range the unwanted reflection at the waveguide grating interface is below  $-24$  dB. The coupler is polarization sensitive; the efficiency for TM polarization is 21 dB lower.

We have also looked at the influence of variations in etch depth and groove width to determine whether the proposed device has reasonable tolerances to fabrication errors. In Fig. 6 the resulting coupling efficiency for different etch depths is shown. For an error of 10 nm the maximum coupling efficiency remains approximately the same but the wavelength is shifted. This wavelength shift can be compensated by adjusting the angle of the fibers, but for most applications the etch depth will have to be controlled accurately. To assess the influence of groove-width errors, we simulated the structure with statistical er-

rors on the width of the grooves (Monte Carlo analysis). When the errors have a normal (Gaussian) distribution with a half-width of  $\sigma = 10$  nm, the resulting coupling efficiency is between 88% and 92%. Also the spectrum is shifted a few nanometers up or down.

In this Letter we have considered only the coupling between a fiber and a 12- $\mu\text{m}$ -wide waveguide. To connect this wide waveguide to a narrow single-mode SOI waveguide, a horizontal spot-size converter is still needed. This can be a simple lateral taper because only horizontal spot-size conversion is needed. Such a taper with a length of 200  $\mu\text{m}$  can achieve a theoretically lossless conversion from a 12- $\mu\text{m}$  to a 500-nm width, but more compact solutions for this problem are also being investigated.

In conclusion, we have proposed an efficient broadband grating coupler for coupling between SOI waveguides and single-mode fibers. When using SOI with a bottom reflector, a coupling loss below 1 dB can be achieved over a 35-nm wavelength range for TE polarization. When using regular SOI with optimized buried oxide thickness, the efficiency is 1.8 dB lower.

Parts of this research were carried out within the context of the European Information Society Technologies Photonic Integrated Circuits Using Photonic Crystal Optics project and the Belgian Interuniversity Attraction Pole PHOTON project. P. Bienstman acknowledges a postdoctoral fellowship from the Flemish Fund for Scientific Research. D. Taillaert's e-mail address is dirk.taillaert@intec.ugent.be.

## References

1. T. Shoji, T. Tsuchizawa, T. Wanatabe, K. Yamada, and H. Morita, *Electron. Lett.* **38**, 1669 (2002).
2. S. J. McNab, N. Moll, and Y. A. Vlasov, *Opt. Express* **11**, 2927 (2003), <http://www.opticsexpress.org>.
3. R. Orobtcouk, A. Layadi, H. Gualous, D. Pascal, A. Koster, and S. Laval, *Appl. Opt.* **39**, 5773 (2000).
4. D. Taillaert, W. Bogaerts, P. Bienstman, T. F. Krauss, and R. Baets, *IEEE J. Quantum Electron.* **38**, 949 (2002).
5. D. L. Lee, *Electromagnetic Principles of Integrated Optics* (Wiley, New York, 1986).
6. P. Bienstman and R. Baets, *Opt. Quantum Electron.* **33**, 327 (2001).
7. E. G. Neumann, *Single-Mode Fibers—Fundamentals* (Springer-Verlag, Berlin, 1988).
8. K. A. Bates, L. Li, R. L. Roncone, and J. J. Burke, *Appl. Opt.* **32**, 2112 (1993).
9. R. Waldhausl, B. Schnabel, P. Dannberg, E. Kley, A. Brauer, and W. Karthe, *Appl. Opt.* **36**, 9383 (1997).
10. J. M. Johnson and Y. Rahmat-Samii, in *Electromagnetic Optimization by Genetic Algorithms*, Y. Rahmat-Samii and E. Michielson, eds. (Wiley, New York, 1999), pp. 1–27.
11. V. A. Sychugov, A. V. Tishchenko, B. A. Usievich, and O. Parriaux, *Opt. Eng.* **35**, 3092 (1996).
12. M. K. Emsley, O. Dosunmu, and M. S. Unlu, *IEEE J. Sel. Top. Quantum Electron.* **8**, 948 (2002).